

# The TICTOP nozzle – first experimental results

Manuel Frey\*, Konrad Makowka\*, Thomas Aichner\*, Ralf Stark\*\* and Chloé Génin\*\*

\*Ariane Group Ottobrunn, 81663 München, Germany

\*\* DLR Lampoldshausen, 74239 Hardthausen, Germany

manuel.frey@ariane.group

## Abstract

In a cold-flow sub-scale nozzle campaign, a thrust-optimized parabolic nozzle (TOP) is compared to two novel TICTOP nozzles that are intended to suppress the formation of the internal shock and the occurrence of restricted shock separation (RSS). Indeed, the shock-free TICTOP nozzle successfully suppresses RSS whereas there is RSS in the TOP nozzle, hence proving the ability of the TICTOP concept to prevent RSS. However, parts of the tests suffer from the occurrence of condensation and desublimation due to high expansion. The TICTOP capability to suppress RSS could only be demonstrated in these cases because RSS did not occur in the TOP nozzle for condensation-free conditions.

## 1. Introduction

Classically, two types of contouring methods have been applied for rocket engine bell nozzles: the truncated ideal contour (TIC) and the thrust-optimized parabola (TOP). The difference between the two becomes obvious especially for sea-level applications where unavoidable flow separation and side-loads occur during the engine start-up. Comparing a TIC and a TOP with the same subsonic contour and the same nozzle exit point (identical length and area ratio), both will deliver the same specific impulse  $I_{sp}$  [1]. However, the TIC will expand to a lower exit wall pressure than the TOP. This means that the TOP nozzle will reach fully attached nozzle flow for lower chamber pressures than the TIC, either resulting in a better margin against steady-state flow separation or enabling to choose a higher area ratio leading to higher performance. On the other hand, the TIC produces a shock-free flow and therefore only shows the well-known free shock separation (FSS) with moderate side-loads during start-up of the engine. In contrast, there is always an internal shock in the TOP, often leading to restricted shock separation (RSS) during start-up, which is feared due to the generation of high side-loads [2].

Recently, a new nozzle contouring type has been proposed, trying to benefit from the advantages of both contouring types and attempting to suppress their drawbacks [1]. Geometrically, the TICTOP concept is a combination of a truncated ideal contour and a parabola. Like the TIC, this new contour type consists of an ideal contour in the upper nozzle part, avoiding the generation of an internal shock. However, starting at a certain transition point where the shape and contour angle remain continuous, the contour continues as a parabola until the nozzle exit as is the case for a TOP, see *Figure 1*. Therefore, the new contouring concept is called TICTOP. Depending on the chosen design Mach number and the axial coordinate of the transition point, some of the possible TICTOP nozzles produce a shock-free flow until the nozzle exit whereas in others, the recompressing character of the parabola produces visible compression or even a shock. Well-designed TICTOP nozzles without recompression promise a shock-free flow without RSS at high exit pressure, combining the positive properties of the two classical bell nozzle contouring concepts. Concerning performance, the specific impulse  $I_{sp}$  of TIC, TOP and TICTOP is identical if the same exit point is used.

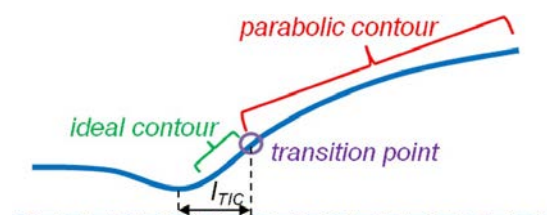


Figure 1: TICTOP nozzle concept, consisting of an ideal contour in the upstream part and a parabolic contour in the downstream part; in the transition point, contour and angle are continuous

In Ref. [1], the principle of the TICTOP nozzle was only proposed on the basis of theoretical considerations. A concept proof via experiments was suggested, but not yet performed. It is the intention of this paper to report about such experimental proof.

The TICTOP concept could be characterized as a "TOP without internal shock and RSS". Therefore, one possibility to experimentally prove the TICTOP concept is to choose an existing TOP nozzle known to produce RSS and redesign it as a TICTOP nozzle. The experimental proof would then consist in showing that the TICTOP with identical exit point and with the same exit wall pressure and  $I_{sp}$  as the TOP does not produce RSS whereas the TOP does. Exactly this has been proposed in Ref. [1] and now serves as a guideline for the work described in this paper.

## 2. Subscale tests at P6.2

As suggested in Ref. [1], the so-called DLR-TOP is applied as reference TOP nozzle for the TICTOP experimental concept proof. This nozzle was used for extensive subscale testing between 1999 and 2001 at DLR Lampoldshausen and showed RSS during start-up and shut-down [2]. As TICTOP nozzle, the contour TICTOP-B1 from Ref. [1] has been chosen that showed to be shock-free in numerical simulations. Its wall pressure gradient  $\partial p_w / \partial x$  is slightly lower than the one of the DLR-TOP, fostering the expectation that side-loads of the TICTOP-B1 should be slightly higher than the ones of the DLR-TOP as long as only FSS is present in the latter. In addition, the contour TICTOP-C2 from Ref. [1] has been chosen, differing from TICTOP-B1 in the choice of design Mach number and transition point location  $l_{TIC}$ . TICTOP-C2 is no longer completely shock-free, but shows some compression waves near the nozzle exit due to the recompressive character of the parabolic contour downstream of the transition point as will later be shown in *Figure 3*. One interesting question for this contour is whether the existing moderate compression is enough to cause RSS. Its wall pressure gradient  $\partial p_w / \partial x$  is slightly higher than the one of the DLR-TOP. *Figure 2* shows the three contours DLR-TOP, TICTOP-B1 and TICTOP-C2. As can be seen, all share the same exit point and substantially only differ in the upstream part of the nozzle, caused by the higher initial contour angle of the DLR-TOP. Having a global look at the contours, DLR-TOP and TICTOP-C2 are quite close to each other whereas TICTOP-B1 is narrower, implying a slightly reduced mass.

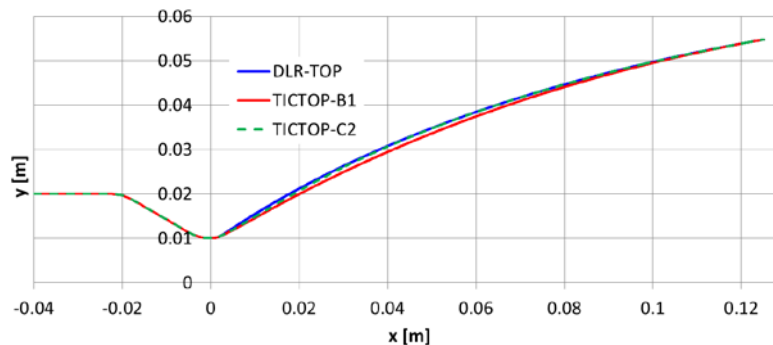


*Figure 2: Comparison of the contours DLR-TOP, TICTOP-B1 and TICTOP-C2 chosen for subscale testing*

Numerical simulations of the three contours have been performed with the RANS-Code Rocflam [4] for full-flowing nozzles (supersonic outflow). In *Figure 3*, Mach number colouring and right-running characteristics are shown. Converging characteristics indicate an internal shock in the DLR-TOP (left) and moderate compression in TICTOP-C2 (centre), whereas the right-running characteristics diverge or are parallel for TICTOP-B1 (bottom), indeed confirming shock-free flow.

For the tests to be performed, DLR Lampoldshausen's P6.2 test facility was chosen [5], [6], where subscale nozzles can be tested at total pressures up to 60 bar. As working fluid, gaseous nitrogen  $N_2$  at ambient temperature is applied in order to suppress condensation effects as far as possible. Although the P6.2 also has an altitude chamber for testing at reduced ambient pressure, all tests were performed outside this chamber, expanding into the ambience. Each performed test consisted of three consecutive increasing-decreasing pressure ramps of different ramp slope, with a chamber pressure below 5 bar in-between. This represents three nozzle start-ups and three shut-downs per run and results in six side-load activities to be evaluated. At the end of the tests, more than 120 of such start-ups and shut-downs have been performed experimentally.

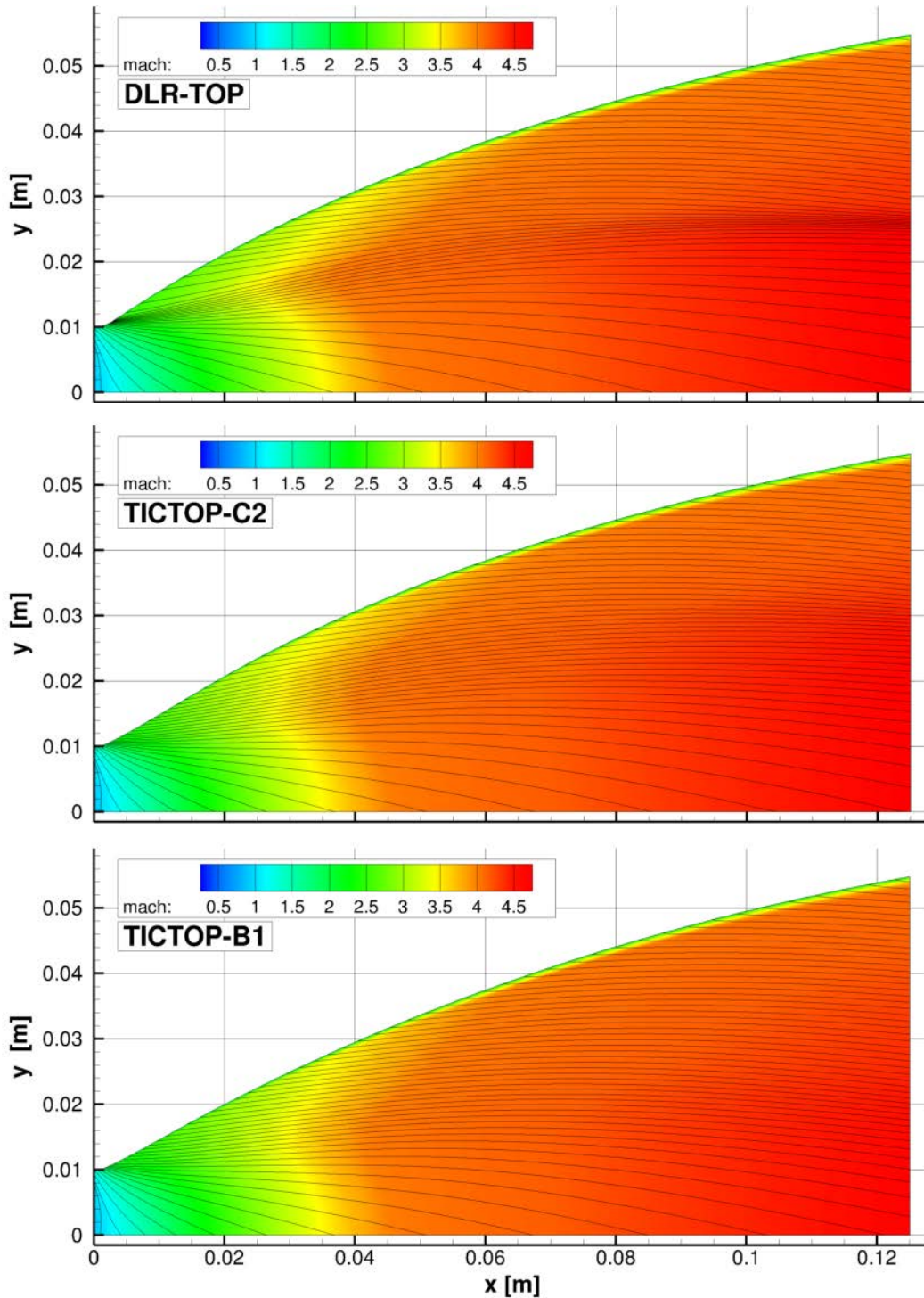


Figure 3: Numerical simulations of the chosen contours using the Navier-Stokes code Rocflam, showing an internal shock in DLR-TOP (top), some compression in TICTOP-C1 (centre) and shock-free flow in TICTOP-B1 (bottom); Mach number colouring and right-running characteristics

All three nozzles were built in acrylic glass with numerous static pressure measurement taps in the nozzle, as can be seen in Figure 4. In addition to pressure measurements, side-loads were determined via strain gauge measurements of the bending tube upstream of the nozzle throat [7]. From this measured system response, the aerodynamic side-loads were computed via a dedicated inertia correction based on dynamic calibration tests applying well-defined forces. Finally, Schlieren images were taken to gather information about the plume behaviour.

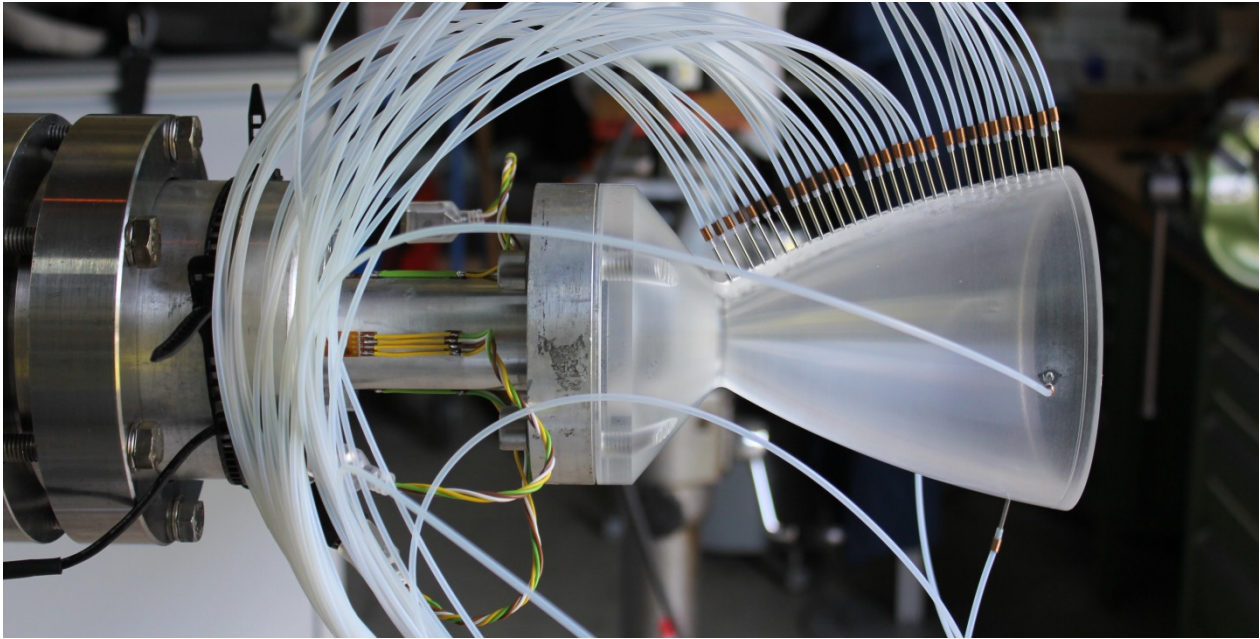


Figure 4: TICTOP-B1 mounted on the P6.2

### 3. Condensation during subscale testing

Already when performing the early DLR-TOP tests between 1999 and 2001, it was well known that condensation or even desublimation of the gaseous nitrogen due to the expansion to cryogenic temperatures could lead to the release of the latent energy of condensation or desublimation. This was known to cause a wall pressure increase, often referred to as "condensation shock". Having in mind that the wall pressure is the most influencing parameter for flow separation, condensation and desublimation can lead to a movement of the flow separation point downstream. Such downstream movement of the separation point promotes the occurrence of RSS [2]. Furthermore, a decreased wall pressure gradient due to condensation or desublimation could lead to higher side-loads following the side-load model established by Schmucker [6].

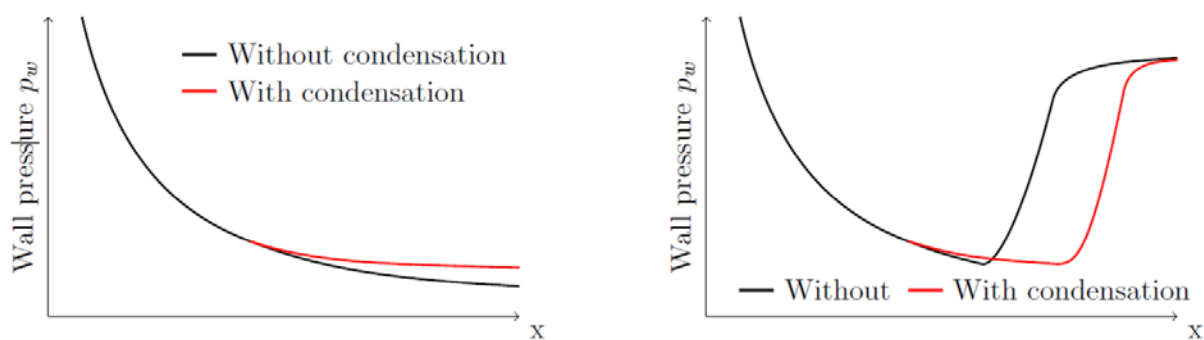
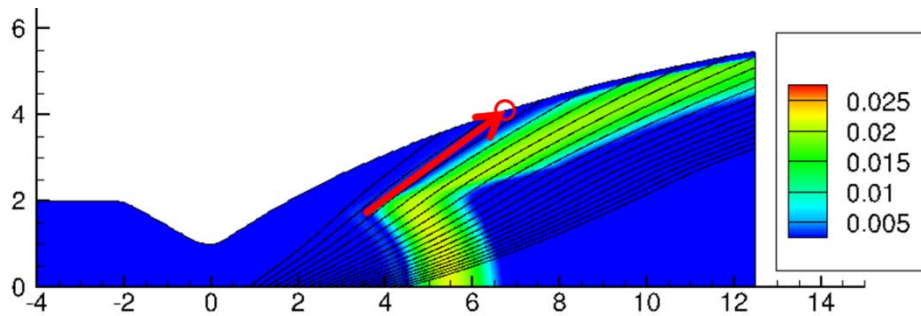


Figure 5: Wall pressure with and without condensation for a fully attached nozzle flow (left) and for a case with flow separation (right), where the separation point moves downstream

For condensing nozzle flows, Oswatitsch [7] differentiates two possible flow behaviours: On the one-hand the wet-isentropic expansion, where the flow condensates as soon as the saturation temperature is reached and on the other hand the dry-isentropic expansion where there is a considerable condensation delay and the flow remains gaseous when passing the saturation temperature. For pure fluids and especially for gaseous nitrogen as applied in the P6.2 tests, Oswatitsch [7] describes a sub-cooling of up to 22K before condensation really occurs, meaning that the gaseous nitrogen condenses considerably later than predicted with equilibrium relations. However, pollution or the presence of gases with a higher condensation temperature such as  $\text{CO}_2$  can destroy this subcooling effect, acting as

nuclei for condensation and leading to a wet-isentropic expansion. Due to this uncertainty in condensation delay it is not simple to predict whether and where condensation occurs in subscale tests.

Numerical simulations taking into account two-phase flow (condensation and desublimation) in an equilibrium wet-isentropic approach show the occurrence of liquid and solid phases for all three nozzles tested at P6.2. The location of wall pressure increase can be found by tracing the left-running characteristic leading through the first occurrence of condensation as shown in *Figure 6*.



*Figure 6: Liquid phase mass fraction in the DLR-TOP together with left running characteristics, both taken from Rocflam simulations; location of wall pressure increase can be found by following the left-running characteristic from the most upstream occurrence of liquid (red arrow)*

Knowing the Rocflam predictions of condensation and desublimation, wall pressure measurements of the new P6.2 tests were carefully investigated to clearly understand the role of condensation and sublimation. And indeed, it was possible to subdivide the ramps in two families -- the first one showing a favourable wall pressure gradient down to the nozzle exit as intended during the nozzle design (green in *Figure 7*), the second one showing an approximately constant wall pressure over the last nozzle section as consequence of condensation and desublimation (red in *Figure 7*). Following the argumentation at the beginning of this section, a flow separation and side-load behaviour representative for flight can only be expected for the first family with only negligible influence of phase change (green in *Figure 7*). In contrast, the flow conditions for the second family (red in *Figure 7*) are clearly deviated, even promoting the occurrence of RSS due to a downstream-shift of the separation location [2]. For all the tests, the first family with flight-representative conditions consists of the first and second start-up, whereas the third start-up and all shutdowns form the second family, hence deviated conditions due to condensation and desublimation.

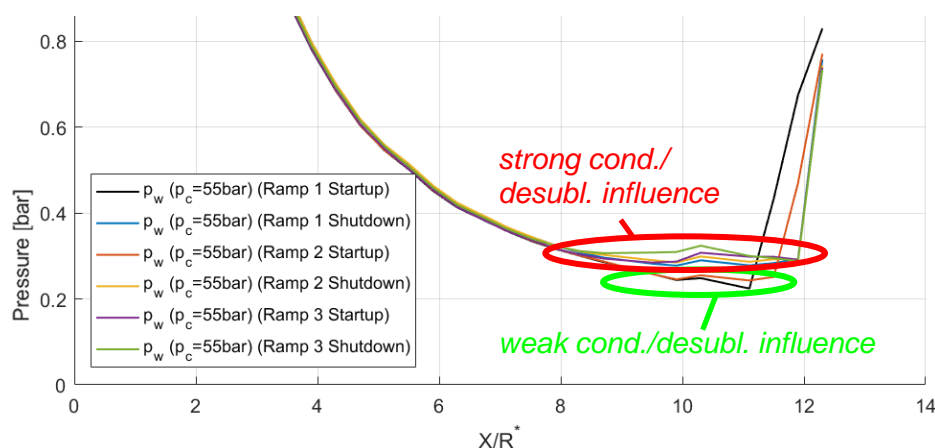


*Figure 7: Exemplary wall pressure for TICTOP-B1 tested at P6.2 for the six different ramps of one test; green family (first two start-ups) shows only weak influence of condensation or desublimation, red family (last start-up, all shutdowns) shows a strong influence*

Generally, the new P6.2 tests show that there is an effect of condensation or desublimation on the wall pressure in some start-ups and shut-downs, which is one of the most important parameters for nozzle flow. Such effects are believed to be even stronger for test facilities using air. Therefore, more focus must be put on avoiding or at least characterizing the influence of condensation or desublimation in future nozzle testing.

## 4. Results

As stated before, all tests were accompanied by high speed Schlieren imaging. Most interesting is to consider the Schlieren images for the highest reached pressures around  $p_c = 60\text{bar}$ , when the overexpansion shock system is fully visible outside the nozzle, see *Figure 8*. For the DLR-TOP, a classical cap shock pattern is observed, confirming the findings from 2000 [2]. For the two TICTOP nozzles B1 and C2, a different shock pattern is observed that has recently been named "Mach lens" [8]. Indeed, the shape resembles a cap shock pattern, but the small strong shock and the cap shock are replaced by a bowed shock of varying strength. However, when analysing these Schlieren images, it must be kept in mind that at this position downstream of the nozzle, it is quite probable to have condensation and desublimation due to the even stronger expansion compared to inside the nozzle. Both the release of the latent heat of condensation or desublimation and the presence of droplets or nitrogen snow flakes may influence the shock patterns. As a further observation, the plume about half a nozzle exit diameter downstream of the nozzle exit plane seems to be narrower for the TICTOP-B1 than for the TICTOP-C2 and DLR-TOP as indicated by white arrows in *Figure 8*. This could be due to the trapped vortex known to exist in the DLR-TOP [9] that is indicated as green lines in *Figure 8*, left. It blocks a part of the plume area and therefore makes the plume larger in diameter. The smaller plume in the TICTOP-B1 may indicate that there is no or only a minor trapped vortex in the TICTOP-B1 nozzle.

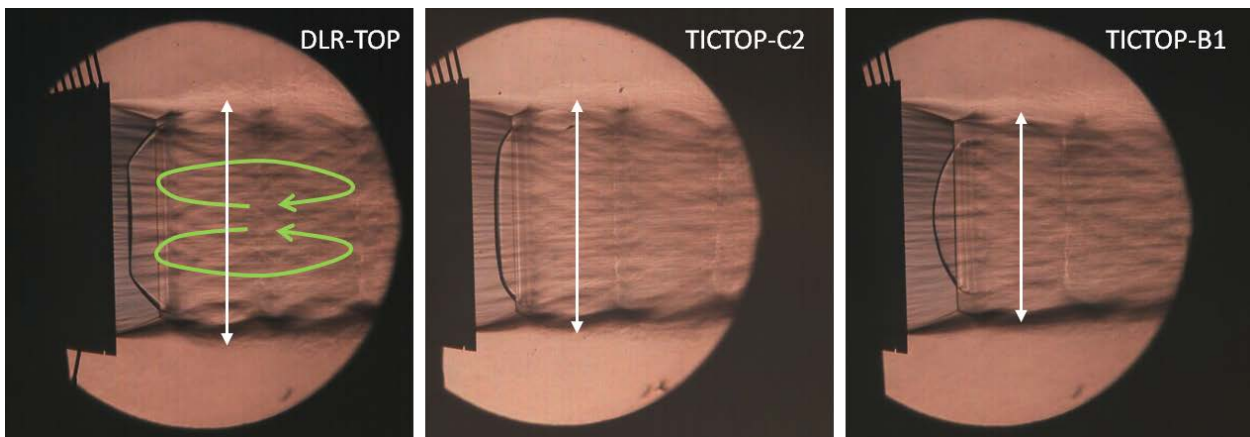


*Figure 8: Schlieren images of the three tested nozzles at P6.2[8]; left: DLR-TOP showing a cap shock pattern, centre and right: TICTOP-C2 and -B1 showing Mach lenses, possibly influenced by condensation and desublimation; white arrows indicate the plume diameter, green lines indicate the trapped vortex known to exist in the DLR-TOP*

### 4.1 Test evaluation for flight-representative conditions

The main task of the P6.2 test campaign is to show that the TICTOP concept successfully suppresses the occurrence of RSS. The necessary evaluation whether FSS or RSS occurs is based on the wall pressure measurements. A transition from FSS to RSS and vice versa is linked to a movement of the separation location. Furthermore, RSS has the peculiarity to produce wall pressure values higher than ambient pressure downstream of the separation point, which is never the case for FSS [2]. This wall pressure behaviour can be used to distinguish FSS from RSS.

The first surprise in the P6.2 test campaign was that in the flight-representative conditions, i. e. during the first two start-up ramps of a test, no RSS occurred at all – neither for the TICTOP nozzles, which was expected, nor for the DLR-TOP, which was in contrast to the observations of the former test campaigns between 1999 and 2001. There is no obvious reason for the deviation of the DLR-TOP behaviour between the old and the new tests, no clear explanation has been identified. However, the old tests were performed inside the P6.2 altitude chamber with varying ambient pressure, whereas the new tests did not use the altitude chamber, hence the nozzle flow expanded always to an ambient pressure of 1 atmosphere. There may be some influence of this difference on the separation location as indicated in Ref. [9]. Anyway, not producing RSS in the DLR-TOP for tests without condensation or desublimation influence precludes the original idea of proving the TICTOP concept in flight-representative conditions.

Still, the side-loads for all flight-representative conditions -- thus for the two first start-ups of all tests -- can be compared for the three nozzles, see *Figure 9*. Although only FSS occurs, the DLR-TOP shows the highest side-loads; TICTOP-B1 and -C2 produce side-loads that are 28% and 26% lower, respectively. Remembering that the wall pressure gradient  $\partial p_w/\partial x$  near the nozzle exit is smallest for TICTOP-B1, this behaviour was not predictable with the Schmucker-like side-load approach mentioned before. Instead, a relation to the width of the plume could be drawn – it can be speculated that during the side-loads activity where flow separation is located inside the nozzle, the proximity of the pulsating shear layer to the wall in the DLR-TOP leads to increased side-loads.

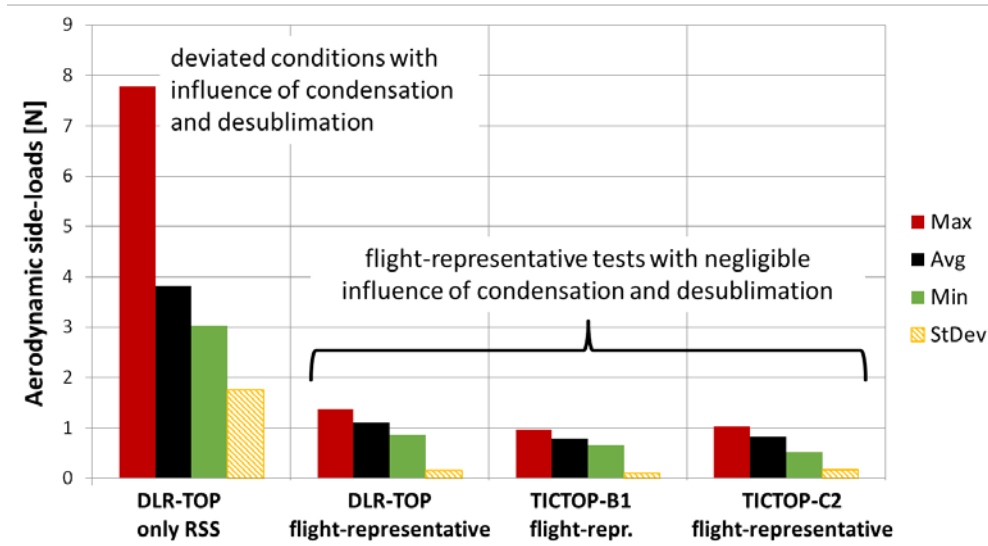


*Figure 9: Side-load data for flight-representative and deviated conditions*

## 4.2 Test evaluation for deviated conditions

In deviated conditions, i. e. with a non-negligible influence of condensation and desublimation on the wall pressure and hence on the separation location, RSS occurred in the DLR-TOP for half of the shutdowns and for one single start-up in the third ramp. In contrast, TICTOP-B2 only showed FSS, and RSS never occurred. This means that the experimental proof of the TICTOP concept, which could not be given in flight-representative conditions, is now given for deviated conditions: Obviously, the non-existence of an internal shock avoided the formation of RSS in spite of the downstream movement of the separation point due to condensation and desublimation. This means that the TICTOP concept indeed works as intended and is able to suppress RSS while keeping the wall exit pressure and  $I_{sp}$  constant.

In the TICTOP-C2 with its moderate compression instead of an internal shock, RSS occurred during two of sixteen shutdowns under deviated conditions. This can be interpreted as a link between the strength of the internal shock and the probability of occurrence of RSS: If there is no internal shock as in TICTOP-B1, there is no RSS. With some moderate compression, some probability of RSS can be observed that increases as a clear internal shock occurs as in DLR-TOP.

The fact that RSS occurred in the TICTOP-C2 but not in -B1 indicates that a TICTOP nozzle must be completely shock-free to suppress RSS. A remaining compression as in the TICTOP-C2 can induce RSS. Therefore, a general design rule for TICTOP nozzles can be deduced stating that any recompression in the nozzle shall be avoided.

The RSS side-loads of the DLR-TOP in deviated conditions are about three times larger than FSS in flight-representative conditions, see *Figure 9*. This confirms earlier findings [2] that side-loads are considerably higher whenever a transition between FSS and RSS occurs. However, it has to be stated that for deviated conditions, also cases with only FSS show some increase in side-load magnitude due to the reduction of wall pressure gradient. This lower gradient allows larger movements of the separation location in FSS, leading to higher side-loads than in the case of flight-like conditions.

## 5. Conclusion

Subscale tests were performed with three different cold-gas sub-scale nozzles at DLR Lampoldshausen's P6.2 test facility. One of the nozzles was the DLR-TOP that had shown the occurrence of RSS earlier. In addition, two different TICTOP nozzles were tested, one of them fully shock-free (B1), the other one with a moderate remaining compression (C2). The aim of the tests was to prove that RSS can be suppressed by the TICTOP design that prevents the formation of an internal shock.

Within the tests, problems with condensation and desublimation occurred for two thirds of the performed pressure ramps, clearly identifiable via an increased wall pressure towards the nozzle exit. It was however possible to subdivide the test data in flight-representative and deviated conditions. Nevertheless, more focus will have to be put on the condensation and desublimation topic for future nozzle tests.

Surprisingly, the DLR-TOP did not show any RSS in flight-like conditions although this had been observed in earlier test campaigns. Therefore, a proof of the TICTOP concept could not be given based on flight-like conditions. Nevertheless, the TICTOP nozzles showed a clear reduction of side-loads by almost 30% compared to the DLR-TOP.

In deviated conditions where condensation and desublimation induce a wall pressure increase, RSS was observed in some tests with the DLR-TOP, but never with the shock-free TICTOP-B1, indicating that the absence of an internal shock indeed suppresses the occurrence of RSS. For the TICTOP-C2 that is not fully shock-free but has some compression near the nozzle exit, RSS also occurred, but with a much lower probability than for the DLR-TOP.

Based on the experimental results in deviated conditions, it can be stated that the TICTOP concept successfully suppresses the formation of RSS with its undesired high side-loads. It is now possible to replace a TOP nozzle by a TICTOP that delivers the same wall exit pressure and the same specific impulse, but does not show RSS. However, the TICTOP concept only works if the nozzle flow is completely shock-free; remaining recompression may lead to the occurrence of RSS.

## Acknowledgement

Parts of this work have been funded by the German Space Agency (Deutsches Zentrum für Luft- und Raumfahrt) DLR within the framework of the research programme TARES, Contract No. 50 RL1210.

## References

- [1] Frey, M., Makowka, K., and Aichner, T. 2016. The TICTOP nozzle: a new nozzle contouring concept. *CEAS Space Journal* Vol. 9, No. 2, 175–181, DOI 10.1007/s12567-016-0139-z
- [2] Frey, M. 2001. Behandlung von Strömungsproblemen in Raketendüsen bei Überexpansion. *Shaker Verlag*, ISBN 3-8265-8806-1
- [3] Frey, M., Stark, R., Ciezki, H., Quessard, F., Kwan, W. 2000. Subscale nozzle testing at the P6.2 test stand. *AIAA2000-3777*
- [4] Frey, M., Kniesner, B., Knab, O. 2011. Considerations of real gas effects and condensation in a spray-combustion rocket-thrust-chamber design tool. *Progress in propulsion physics* Vol. 2, EUCASS book series, ISBN 978-2-75980673-7
- [5] Kronmüller, H., Schäfer, K., Zimmermann, H. and Stark R. 2002. Cold Gas Subscale Test Facility P6.2 at DLR Lampoldshausen. *6th Symposium on Propulsion for Space Transportation of the XXIst century*, Palais des Congres, Versailles, France
- [6] Schäfer, K., Böhm, C., Kronmüller, H., Stark, R. and Zimmermann H. 2005. P6.2 Cold Gas Test facility for Simulation of Flight Conditions - Current Activities. *EUCASS, 1st European Conference for Aerospace Sciences*, Moscow, Russia
- [7] Stark, R., and Génin, C. 2015. Parametrical Study on Side Load Generation in Subscale Rocket Nozzles, *EUCASS, 6th European Conference for Aerospace Sciences*, Kraków, Poland



- [8] Schmucker, R. 1973. Strömungsvorgänge beim Betrieb überexpandierter Düsen chemischer Raketentriebwerke, Teil 2: Seitenkräfte durch unsymmetrische Ablösung. *Bericht TB-10, Technische Universität München*
- [9] Stark, R. and Génin, C. 2017. Flow Separation in Rocket Nozzles under High Altitude Condition. *Shock Waves*, Vol. 27, Issue 1, 63–68, DOI 10.1007/s00193-016-0631-6
- [10] Oswatitsch, K. 1976: Grundlagen der Gasdynamik, *Springer Verlag Wien*, ISBN 978-3-7091-8416-5
- [11] Stark, R. and Génin, C. 2017. Experimental Study of TICTOP Nozzles. *31th International Symposium on Shock Waves (ISSW31)*, Nagoya, Japan
- [12] Kwan, W., Stark, R. 2002. Flow separation phenomena in subscale rocket nozzles. *AIAA2002-4229*